

# Nuclear Accumulation of Truncated Atrophin-1 Fragments in a Transgenic Mouse Model of DRPLA

Gabriele Schilling,<sup>1,10</sup> Jonathan D. Wood,<sup>1,10</sup> Kui Duan,<sup>1</sup> Hilda H. Slunt,<sup>2</sup> Vicky Gonzales,<sup>2</sup> Mitsunori Yamada,<sup>7</sup> Jillian K. Cooper,<sup>1</sup> Russell L. Margolis,<sup>1</sup> Nancy A. Jenkins,<sup>6</sup> Neal G. Copeland,<sup>6</sup> Hitoshi Takahashi,<sup>7</sup> Shoji Tsuji,<sup>8</sup> Donald L. Price,<sup>2,3,4</sup> David R. Borchelt,<sup>2,9</sup> and Christopher A. Ross<sup>1,3,5,9</sup>

<sup>1</sup>Division of Neurobiology

Department of Psychiatry

<sup>2</sup>Department of Pathology and

Division of Neuropathology

<sup>3</sup>Department of Neuroscience

<sup>4</sup>Department of Neurology

<sup>5</sup>Program in Cellular and Molecular Medicine

The Johns Hopkins University School of Medicine

Baltimore, Maryland 21205

<sup>6</sup>Mammalian Genetics Laboratory

National Cancer Institute Cancer Center

Frederick, Maryland 21702

<sup>7</sup>Department of Pathology

<sup>8</sup>Department of Neurology

Brain Research Institute

Niigata University

Niigata 951

Japan

## Summary

Dentatorubral and pallidoluysian atrophy (DRPLA) is a member of a family of progressive neurodegenerative diseases caused by polyglutamine repeat expansion. Transgenic mice expressing full-length human atrophin-1 with 65 consecutive glutamines exhibit ataxia, tremors, abnormal movements, seizures, and premature death. These mice accumulate atrophin-1 immunoreactivity and inclusion bodies in the nuclei of multiple populations of neurons. Subcellular fractionation revealed 120 kDa nuclear fragments of mutant atrophin-1, whose abundance increased with age and phenotypic severity. Brains of DRPLA patients contained apparently identical 120 kDa nuclear fragments. By contrast, mice overexpressing atrophin-1 with 26 glutamines were phenotypically normal and did not accumulate the 120 kDa fragments. We conclude that the evolution of neuropathology in DRPLA involves proteolytic processing of mutant atrophin-1 and nuclear accumulation of truncated fragments.

## Introduction

Dentatorubral and pallidoluysian atrophy (DRPLA) is an autosomal dominant progressive neurodegenerative disorder that usually manifests in midlife. The symptoms

of DRPLA are similar to those of Huntington's disease (HD) and include chorea (and other involuntary movements), ataxia, incoordination, and dementia (Smith et al., 1958; Naito and Oyanagi, 1982; Ross et al., 1997a, 1997b). The disease is caused by an expansion of a highly polymorphic CAG repeat in the coding region of the *atrophin-1* gene. The repeat length for *atrophin-1* ranges from 6 to 35 CAG repeats in unaffected individuals and from 49 to 88 CAG repeats in DRPLA cases (Koide et al., 1994; Nagafuchi et al., 1994a). Juvenile cases of DRPLA, which are associated with expansions >60 CAG repeats, tend to show fewer involuntary movements and have a high incidence of seizures (Ross et al., 1997b).

Neuropathological characteristics of the disease are loss of neurons and gliosis in several areas of the brain, including the dentate nucleus of the cerebellum, red nucleus, globus pallidus, and subthalamic nucleus (Naito and Oyanagi, 1982; Iizuka et al., 1984; Takahashi et al., 1988; Becher et al., 1997; Ross et al., 1997a, 1997b). These neurons, as well as many other populations of neurons, show ubiquitin-immunoreactive nuclear inclusion bodies (Becher et al., 1998; Hayashi et al., 1998; Igarashi et al., 1998).

DRPLA and HD are members of a growing family of polyglutamine repeat diseases that also include spinal and bulbar muscular atrophy and several forms of spinocerebellar ataxia (The Huntington's Disease Collaborative Research Group, 1993; Orr et al., 1993; Banfi et al., 1994; Koide et al., 1994; Nagafuchi et al., 1994b; Gusella and MacDonald, 1996; Paulson and Fischbeck, 1996). These diseases share many common features, such as anticipation, repeat instability, and widespread expression of the gene product, with neuronal loss restricted to distinct subsets of neurons. DRPLA patients (like patients with the other diseases) show restricted neurodegeneration despite widespread expression of the gene product in the brain and peripheral tissues (Nagafuchi et al., 1994a; Margolis et al., 1996).

The *atrophin-1* gene was initially cloned as CTG-B37 by screening of brain cDNA libraries for CAG repeats (Li et al., 1993). It encodes a protein, atrophin-1, with a calculated molecular mass of 125 kDa and an apparent molecular mass of ~200 kDa on SDS-PAGE (Yazawa et al., 1995; Miyashita et al., 1997; Wood et al., 1998). Atrophin-1 contains several regions with simple repetitive sequences, including a serine-rich region, a polyproline tract, and a region of alternating acidic and basic residues, in addition to the polyglutamine repeat. Atrophin-1 has been reported to have cytoplasmic and nuclear distributions in neurons (Yazawa et al., 1995).

To examine the biology of mutant atrophin-1 in vivo, we have now generated transgenic mouse lines expressing full-length atrophin-1 with 65 or 26 glutamines (AT-FL-65Q and AT-FL-26Q, respectively). Expression of the transgene was driven by the mouse prion protein promoter, which expresses in a copy number-dependent and integration site-independent manner in CNS neurons and some peripheral tissues (Borchelt et al., 1996). Several lines of AT-FL-65Q mice showed a

<sup>9</sup>To whom correspondence should be addressed (e-mail: caross@jhu.edu [C. A. R.], drbor@welchlink.welch.jhu.edu [D. R. B.]).

<sup>10</sup>These authors contributed equally to this work.

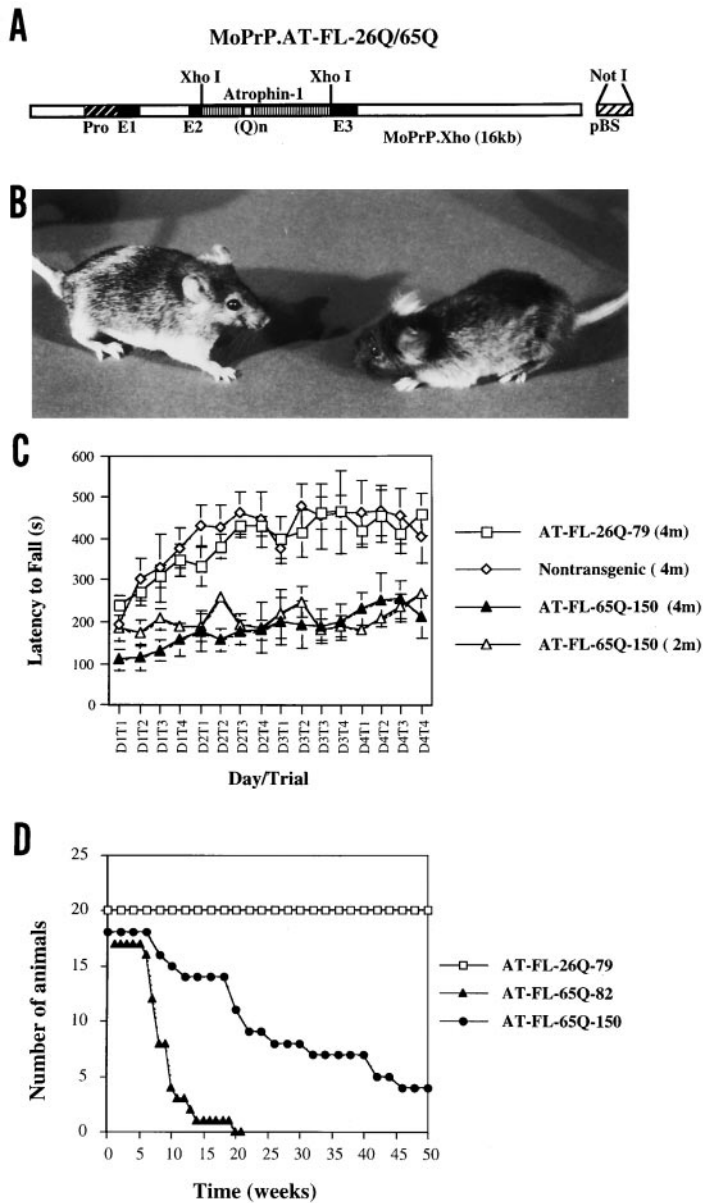


Figure 1. Phenotypic Analysis of DRPLA Transgenic Mice

(A) Vector map of MoPrP.AT-FL-26Q/65Q. Full-length *atrophin-1* cDNAs (with no epitope tags) encoding 26 or 65 consecutive glutamines ((Q)n) were flanked with XhoI linkers and subcloned into the mouse prion protein promoter (Pro) vector (MoPrP.Xho). The non-coding portions of the second and third exons (E2 and E3) of the *PrP* gene were fused into one exon that contains the *atrophin-1* cDNA insert (with its own start and stop codons). The genomic *PrP* sequences are cloned into the NotI site of pBluescript SK<sup>+</sup> (pBS).

(B) Long exposure photograph of a 6.5-month-old AT-FL-65Q-150 mouse and an age-matched AT-FL-26Q-79 mouse, illustrating the resting tremor seen in AT-FL-65Q mice. Other phenotypic characteristics include jerky movements, ataxic gait, low weight, seizures, hindlimb claspings, poor breeding, and premature death.

(C) Rotating rod analysis showing that the performance of AT-FL-65Q-150 mice at 4 months of age was very impaired compared with age-matched AT-FL-26Q-79 mice and nontransgenic mice.

(D) Death curves for AT-FL-65Q-82, AT-FL-65Q-150, and AT-FL-26Q-84, illustrating premature death of mutant transgenic mice.

progressive neurological phenotype that includes ataxia, involuntary movements, tremors, seizures, and premature death. The brains of affected mice contained accumulations of atrophin-1 immunoreactivity in the nuclei of multiple populations of neurons, including the dentate nucleus and granular layer of the cerebellum, cochlear nucleus, pons, regions of basal ganglia, and cortex. The nuclei of most neurons exhibiting nuclear staining also contained atrophin-1-immunoreactive inclusions. The temporal and spatial distribution of the nuclear immunoreactivity in the mice correlated well with the appearance and accumulation of 120 kDa fragments of mutant atrophin-1. Furthermore, apparently identical mutant atrophin-1 fragments were present in the brains of DRPLA cases. We conclude that the evolution of pathological changes in DRPLA involves proteolytic processing of mutant atrophin-1 to generate fragments that preferentially accumulate and aggregate in the nucleus. This work represents a definitive example of proteolytic

processing and accumulation of the mutant polyglutamine protein as pathologic mechanisms in a transgenic mouse model of a trinucleotide repeat disorder.

## Results

### DRPLA 65Q Mice Exhibit a Progressive Neurological Phenotype

We generated transgenic mice that express full-length human atrophin-1 with 26 glutamines (normal, AT-FL-26Q) and 65 glutamines (mutant, AT-FL-65Q) under the transcriptional control of the mouse prion protein promoter, which expresses in neurons throughout the brain (Borchelt et al., 1996) (Figure 1A). Thirty-eight AT-FL-65Q founders were obtained, several of which showed frequent seizures and died prematurely. Nevertheless, we were able to establish several lines of AT-FL-65Q mice in which levels of expression and behavioral phenotypes were examined. Only AT-FL-26Q founders with

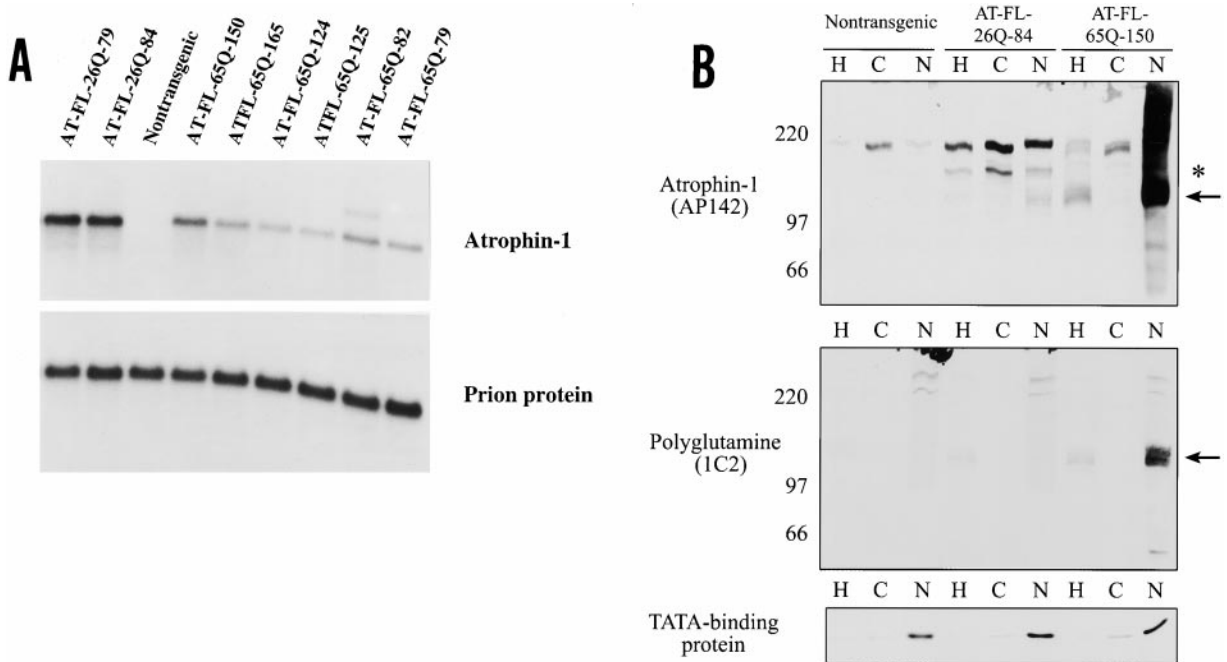


Figure 2. Transgene Expression of DRPLA Transgenic Mice

(A) Northern blot analysis of transgene expression in transgenic lines. The highest expression of the transgene mRNA was seen in the control lines AT-FL-26Q-79 and AT-FL-26Q-84. Several-fold lower expression of mRNA was observed in the mutant lines AT-FL-65Q-79, AT-FL-65Q-82, and AT-FL-65Q-150. These three mutant lines showed a similar early onset phenotype before 2 months. Lower expressing AT-FL-65Q lines (124, 125, and 165) gave late symptoms (onset, 8–12 months of age). Endogenous mouse *atrophin-1* mRNA was not detected at the hybridization stringency used. The blot was reprobbed with a fragment of the mouse prion protein cDNA to verify equal loading of RNA in each lane (lower panel).

(B) Immunoblot analysis of total homogenates (H), cytosol (C), and preparations enriched in nuclei (N) from age-matched nontransgenic, AT-FL-26Q-84, and AT-FL-65Q-150 mouse brains. The equivalence of loading was confirmed by Coomassie blue staining of an identically loaded gel (data not shown). This gel also confirmed the efficiency of separation of nuclear and cytoplasmic proteins into the different subcellular fractions. The upper panel shows an immunoblot probed with the anti-atrophin-1 antibody AP142. In nontransgenic mouse brain samples, atrophin-1 was highly enriched in the cytosol but was also present in the fraction enriched in nuclei. Homogenates from AT-FL-65Q-150 contained distinct 120 kDa fragments (indicated with an arrow), in addition to full-length endogenous mouse and transgene-derived human atrophin-1. The 120 kDa fragments were highly enriched in the nuclear fraction, while full-length atrophin-1 polypeptides predominated in the cytosol. Note the smearing of atrophin-1 immunoreactivity in the nuclear fraction, indicative of aggregation. Comparison of full-length atrophin-1 levels in AT-FL-26Q-84 and AT-FL-65Q-150 homogenates and cytosol demonstrates that protein expression is higher in the wild-type than in the mutant transgenic mice, in agreement with the Northern blot data. Full-length atrophin-1 predominated in AT-FL-26Q-84 nuclei and cytosol, although a prominent 150 kDa band (marked with an asterisk) was observed, and there was also faint immunoreactivity around 120 kDa in the nuclear fraction. The middle panel shows an identically loaded immunoblot probed with the expanded polyglutamine-specific monoclonal antibody 1C2. The 120 kDa fragments (indicated with an arrow) are detected with 1C2, confirming that they contain the expanded polyglutamine tract. The lower panel shows an immunoblot probed with an anti-TBP antibody (N-12; Santa Cruz Biotechnology) to confirm enrichment of nuclear proteins in the nuclear preparations.

the highest numbers of transgene copies were bred, and we have maintained a number of lines of mice that have the highest levels of transgene-derived mRNA (see below). AT-FL-26Q mice have remained indistinguishable from nontransgenic littermates for more than 18 months.

Mice expressing AT-FL-65Q (lines 79, 82, and 150) exhibited a progressive phenotype consisting of involuntary tremors (Figure 1B), ataxic gait, and loss of coordination (Figure 1C), consistent with dysfunction of the cerebellum (and other brain regions), beginning at 1–2 months of age. The 65Q mice showed other behavioral signs, including hyperactivity, increased aggression, and lower breeding efficiency. The phenotypes were consistent among the different lines of mice, with the only variable being the age of onset. Death curves (Figure 1D) illustrate premature death of AT-FL-65Q lines 82 and 150, compared with AT-FL-26Q controls. Seizures

were observed in some animals, particularly in lines 82 and 150, and may contribute to premature death. Overall, the behavioral phenotype of the mice closely resembles that of the human disease. Adult DRPLA patients show involuntary movements (including chorea and intention tremors), ataxia, and dementia (Smith et al., 1958; Naito and Oyanagi, 1982), and juvenile onset DRPLA patients often have seizures (Ross et al., 1997a, 1997b). The length of the polyglutamine tract in our mice is typical of that seen in juvenile cases (Koide et al., 1994; Ikeuchi et al., 1995; Komure et al., 1995).

#### Expression of Normal and Expanded Atrophin-1 in Transgenic Mice

Northern blot analysis of transgene-derived mRNA levels (Figure 2A) indicated that mice expressing AT-FL-26Q (lines 79 and 84) showed the highest levels of

expression, greater than that in mice expressing AT-FL-65Q (lines 79, 82, and 150). A signal for endogenous mouse *atrophin-1* mRNA was not detected at the hybridization stringency used. These Northern blots demonstrate a single transgene mRNA species. The onset of symptoms correlated well with the levels of mutant mRNA. Mice expressing lower levels of mutant atrophin-1 (lines 124, 125, and 165; see Figure 2A) developed symptoms at about 8–12 months of age, whereas mice expressing higher levels (lines 79, 82, and 150) developed symptoms between 1 and 2 months of age.

#### Nuclear Localization and Proteolytic Processing of 65Q Atrophin-1

To assess the subcellular distribution of 26Q and 65Q atrophin-1 protein in the brains of these animals, total homogenates, cytosol, and nuclei were prepared from nontransgenic, AT-FL-26Q-84, and AT-FL-65Q-150 mouse brains and analyzed by immunoblotting with the anti-atrophin-1 antibody AP142 (Wood et al., 1998) (directed against residues 425–439, which are 100% conserved between mouse and human; Figure 2B, upper panel). Comparison of full-length atrophin-1 immunoreactivity in total homogenates (Figure 2B, upper panel, lanes 1, 4, and 7) suggests that AT-FL-26Q-84 mice express five to ten times the level of endogenous atrophin-1, while AT-FL-65Q-150 mice (the line most extensively analyzed in the present study) appeared to express a level comparable to that of endogenous atrophin-1. The lower levels of transgene-derived mRNA in the AT-FL-65Q-150 mice as compared with either of the two lines of AT-FL-26Q mice (see Figure 2A) support the idea that the levels of mutant protein expression are lower than the AT-FL-26Q expression levels. Assessing the total level of transgene products in these animals is difficult, as both 26Q and 65Q atrophin-1 are subject to proteolytic processing. Moreover, the abundance of the 120 kDa fragments in the 65Q mice increases with age (see below). On the basis of the relative abundance of the full-length transgene-derived protein levels, we conclude that the line 150 mice express a level comparable to or slightly greater than that of endogenous atrophin-1.

Subcellular fractionation studies of total brain homogenates demonstrated that both endogenous and human 26Q atrophin-1 were predominantly cytosolic, with a smaller fraction detected in preparations enriched for nuclei (Figure 2B). In mice expressing high levels of human 26Q atrophin-1, there were proteolytic fragments of the normal protein, with the predominant species showing an apparent mass of 150 kDa and a minor species of 120 kDa. In cell transfection experiments, a 150 kDa band is always apparent when normal and expanded forms of atrophin-1 are overexpressed (Wood et al., 1998). The larger fragments were largely localized to the cytosol (Figure 2B, upper panel, asterisk). Small amounts of 120 kDa fragment were present in the nuclear fraction of mice expressing AT-FL-26Q. In 65Q (line 150) mice, both full-length mutant protein and proteolytic fragments were detected; the prominent proteolytic fragments showed a relative mass of 120 kDa and were entirely localized to the nucleus (Figure 2B). Immunoblotting with an antibody specific for expanded polyglutamine tracts (1C2) (Trottier et al., 1995) demon-

strated that in the mutant mice, the fragments contained the expanded glutamine tract (Figure 2B, middle panel). These fragments were also recognized by an antibody to the N terminus (residues 1–15) of atrophin-1 (data not shown).

#### Intranuclear Inclusions and Diffuse Nuclear Labeling in Mutant Atrophin-1 Mice

Histological analysis of several severely affected, 12-month-old 65Q mice did not reveal abnormalities in peripheral tissues, including liver, pancreas, kidney, lung, and skeletal muscle. Although there were a few intranuclear inclusions in heart (data not shown), a tissue in which the prion promoter expresses well, histological preparations of heart were normal. Inclusions were absent in skeletal muscle (data not shown). The resting blood glucose levels in 12-month-old 65Q mice were normal (baseline glucose levels were measured at  $154 \pm 23$  and  $169 \pm 23$  mg.dl<sup>-1</sup> in 13-month-old AT-FL-65Q-150 mice [ $n = 4$ ] and age-matched nontransgenic controls [ $n = 3$ ], respectively).

Overall, the brains of the AT-FL-65Q transgenic mice appeared to be grossly normal. In the brains of several endstage mice, there did not appear to be increased labeling for glial fibrillary acidic protein, indicating that there was no reactive gliosis. Silver impregnation indicated a normal cytoskeletal architecture (data not shown).

However, immunohistochemical staining of symptomatic AT-FL-65Q brain with AP142 revealed diffuse nuclear staining of variable frequency and intensity throughout the brain (Figures 3A–3K), similar to what is seen in DRPLA patients (Becher et al., 1997; Hayashi et al., 1998). In our AT-FL-65Q mice, nuclei in the cerebellum and cortex showed very strong immunoreactivity (Figures 3A–3C and 3J), whereas relatively few nuclei in striatum (Figure 3G), olfactory bulb (Figure 3K), and brainstem (Figure 3E) were immunoreactive with AP142. The immunoreactivity in the cerebellar dentate nucleus of two independent AT-FL-65Q lines (lines 82 and 150) exhibited similar nuclear labeling and inclusions (Figures 4A and 4C). All atrophin-1 immunoreactivity could be competed out completely by preincubation with the peptide antigen (Figures 4B and 4D). Nuclear immunostaining was much less intense in mice expressing AT-FL-26Q (Figure 4E), even though these mice express higher levels of mRNA and protein than the mutant mice (see Figure 2A). Nontransgenic mice exhibited diffuse nuclear and cytoplasmic labeling (Figure 4F), consistent with the results from subcellular fractionation (see Figure 2B).

Intranuclear inclusions in DRPLA postmortem brain were detectable with an anti-ubiquitin antibody (Becher et al., 1998; Hayashi et al., 1998; Igarashi et al., 1998). In contrast, immunostaining of paraffin sections from endstage AT-FL-65Q mouse brain with two different anti-ubiquitin antibodies did not reveal intranuclear inclusions (data not shown). It is possible that the epitope was hidden in mouse brains or that ubiquitination occurs very late in the disease.

Neuropil aggregates have been observed in several areas of brain from HD patients and HD transgenic mouse models (DiFiglia et al., 1997; Reddy et al., 1998; Gutekunst et al., 1999; Schilling et al., 1999). Immunostaining with our atrophin-1 antibody failed to recognize

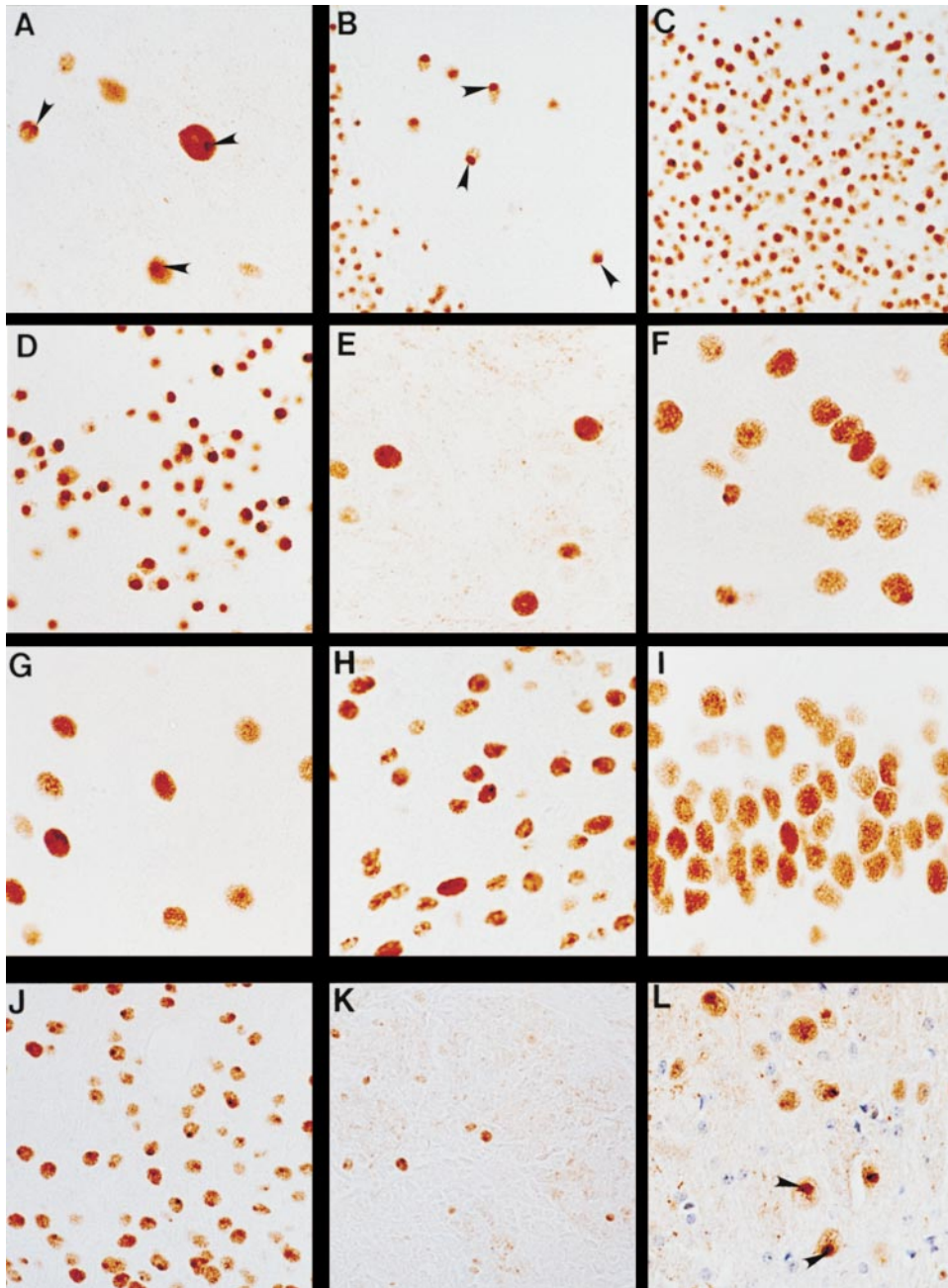


Figure 3. Intense Diffuse Nuclear Staining and Intranuclear Inclusion Bodies in Different Brain Regions of AT-FL-65Q Mice

Immunostaining of sections of paraffin-embedded brains of AT-FL-65Q F3 offspring with AP142 (1:10,000) demonstrated intense diffuse nuclear staining and a high density of nuclear inclusions in the dentate nucleus (A), molecular cell layer (B), and granule cell layer (C) of the cerebellum, as well as in cochlear nucleus (D), thalamus (F), amygdala (H), hippocampus (I), and cortex (J). Inclusions were less frequent or absent in the brainstem (E), striatum (G), and olfactory bulb (K). The polyglutamine antibody 1C2 detected inclusions in an endstage founder in the trigeminal nucleus of the brainstem (L). (A), (B), (C), (D), and (H) are from a 4.5-month-old AT-FL-65Q-82 animal, while (E), (F), (G), (I), (J), and (K) are from a 9-month-old AT-FL-65Q-150 animal. Original magnification was 263 $\times$  for (A) through (G) and 160 $\times$  for (J) through (L).

neuropil aggregates in 65Q mouse brain sections, when analyzed by light microscopy, suggesting that aggregation might be a solely nuclear event.

To determine the relationship between nuclear staining, nuclear inclusions, and atrophin-1 processing, we examined the temporal and spatial distribution of mutant atrophin-1 fragments. Nuclei were prepared from AT-FL-65Q-150 brains at several different time points and analyzed

by immunoblotting and immunostaining with AP142. Data from 1-month-old and 11-month-old animals are shown in Figure 5. Between 1 and 11 months of age, there was a dramatic increase in the levels of the 120 kDa fragments (Figure 5A). There was also marked increase in high molecular weight-immunoreactive species, which may represent aggregated or modified species of the mutant fragments. The 11-month-old animals

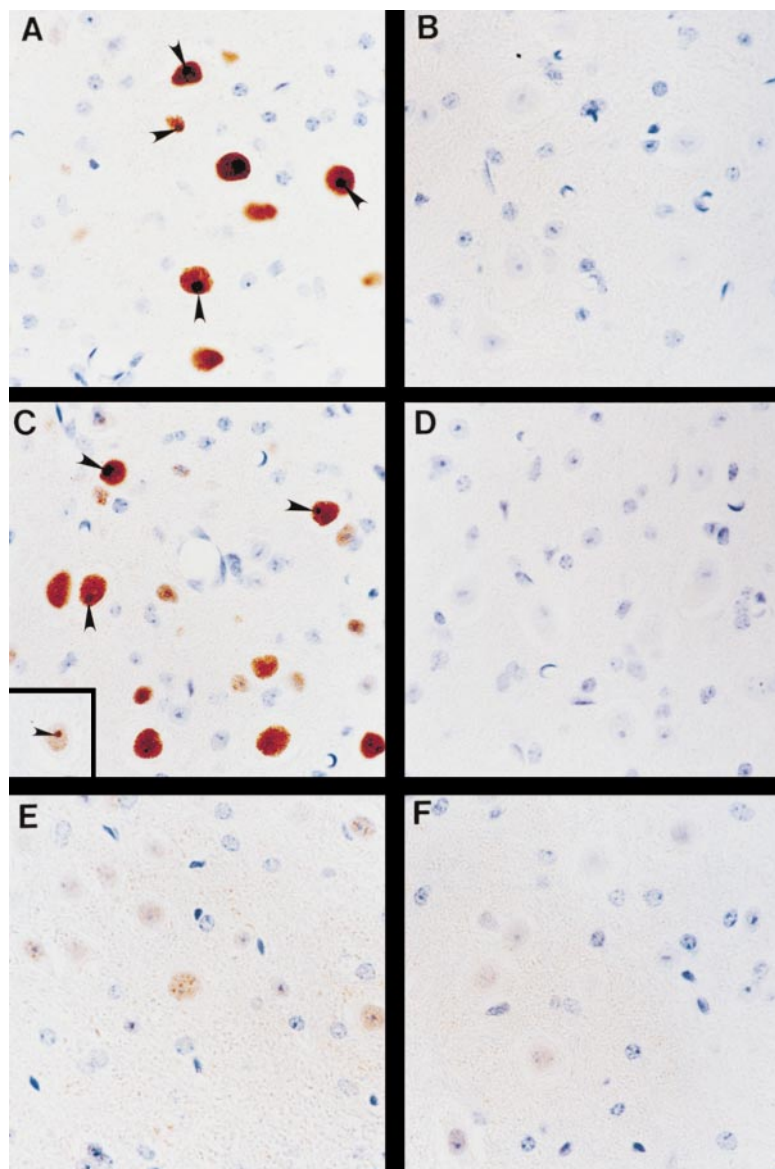


**Figure 4. Atrophin-1 Localization in the Dentate Nucleus of the Cerebellum**

Immunohistochemical staining of sagittal sections of paraffin-embedded tissue with the polyclonal, anti-peptide antibody AP142 (1:10,000) reveals intense nuclear staining and dense intranuclear inclusion bodies (marked by arrowheads), in the dentate nucleus of the cerebellum in lines AT-FL-65Q-82 (4.5 m) (A) and AT-FL-65Q-150 (9 m) (C). The inset shows that the inclusion bodies in the dentate nucleus are more readily visualized by further dilution of the antibody to 1:25,000. All of the staining in lines AT-FL-65Q-82 (B) and AT-FL-65Q-150 (D) was abolished by preincubation of AP142 with the corresponding peptide antigen, demonstrating that the diffuse nuclear immunostaining represents specific labeling. Staining of equivalent sections from the control line AT-FL-26Q-79 (E) revealed a combination of general cytoplasmic and punctate nuclear staining but no nuclear inclusion bodies that are distinct from nucleoli or chromatin fragments (small dark blue structures in some nuclei). Little or no atrophin-1 immunoreactivity was detected in nontransgenic mice under the conditions optimal for visualizing the antigen in mutant transgenic mice (F). Original magnification was 263 $\times$ . Obvious neuronal loss was not observed in the dentate nucleus of the cerebellum. It is possible that small losses (20%–30%) may have occurred. Stereologic cell counts on multiple animals will be required to determine the extent of cell loss.

show severe tremor and ataxia, while the 1-month-old animals show no tremor or ataxia. Immunocytochemical stains of 1- and 11-month-old animals show that the relative frequency of immunostained nuclei increases in concert with the increase in the level of the mutant protein (data not shown). An examination of the regional distribution of the 120 kDa fragments in P1 fractions of brains from symptomatic AT-FL-65Q-150 (Figure 5B) demonstrated a direct correlation with the distribution of diffuse nuclear atrophin-1 immunoreactivity seen in immunohistochemical analyses (see Figure 3). In cerebellum and cortex, which show very intense nuclear immunostaining, the 120 kDa fragments were more abundant than the full-length transgene protein. The region with the highest level of 120 kDa fragments was the cerebellum. In olfactory bulb and brainstem, where fewer nuclei showed intense nuclear immunostaining, the levels of the 120 kDa fragments were relatively low. Collectively, these data strongly suggest that the nuclear immunostaining

seen in the 65Q mice is a consequence of the generation and accumulation of the 120 kDa fragments.

#### Proteolytic Processing of Atrophin-1 in DRPLA Patients

To determine whether the accumulation of truncated atrophin-1 products could be relevant to the human condition, enriched nuclear fractions were prepared from frozen pieces of human DRPLA and non-DRPLA cerebella. On immunoblot analysis with AP142, a banding pattern similar to that seen in AT-FL-65Q mice was observed, including the 120 kDa fragments, high-molecular weight (>200 kDa) bands, and high-molecular weight smearing, which began at around 120 kDa, as in AT-FL-65Q mouse brain samples (Figure 6). In control cases, a single band around 200 kDa was observed. Immunoblotting with 1C2 confirmed that the 120 kDa fragments contained the expanded polyglutamine tract (data not shown). Diffuse nuclear labeling, similar to that observed in AT-FL-65Q

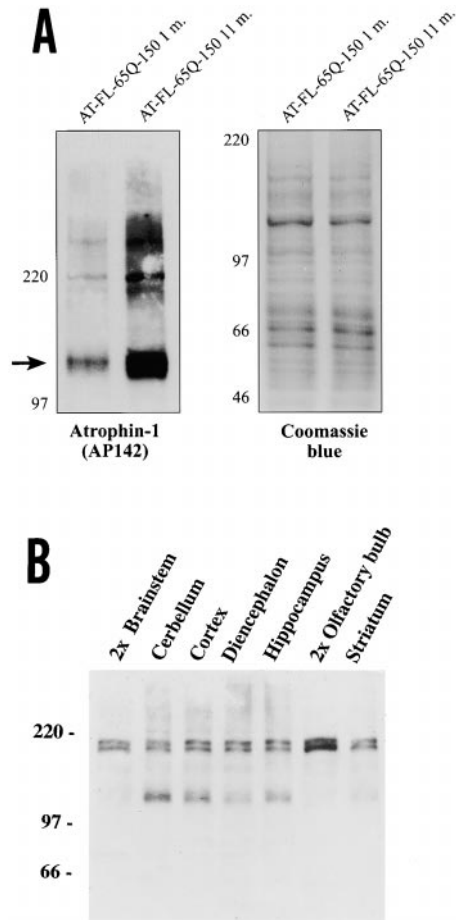


Figure 5. Temporal Accumulation of 120 kDa Fragments in AT-FL-65Q-150 Brain

(A) Nuclei were prepared from the whole brains of individual mice and analyzed by immunoblotting for atrophin-1. The 120 kDa fragments were detected in nuclei from the 1-month-old animal (indicated with an arrow) but were much more abundant in nuclei from the 11-month-old animal. Equivalence of loading was confirmed by Coomassie blue staining of an identically loaded gel (right panel). (B) Regional distribution of 120 kDa atrophin-1 fragments in AT-FL-65Q-150 mouse brains. Three mouse brains were dissected, specific regions were pooled, and P1 fractions were prepared as described in the Experimental Procedures. Protein (20  $\mu$ g) was loaded to each lane, except for brainstem and olfactory bulb, where 40  $\mu$ g was loaded. The 120 kDa fragments were most prominent in cerebellum and least prominent in brainstem and olfactory bulb, even with double the loading compared with the other regions.

mice, was observed in postmortem DRPLA brains in cerebellar dentate nucleus, granule cells, and pons (H. Yamada, personal communication). These data demonstrate that truncated fragments of mutant atrophin-1 are found in the nuclei of DRPLA patients. The lower levels of the 120 kDa fragments in the patients may reflect difficulties in subcellular fractionation of human post-mortem tissue or a loss of affected neurons.

## Discussion

We demonstrate that transgenic mice expressing mutant human atrophin-1 develop a neurologic disorder,

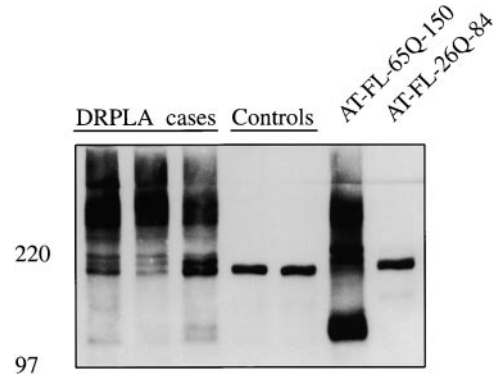


Figure 6. Immunoblot Analysis of Nuclear Protein Extracts from Human Cerebellar Cortex Samples and Whole Transgenic Mouse Brains

Seemingly identical 120 kDa fragments were seen in the DRPLA patient and in AT-FL-65Q transgenic mouse samples. Shorter exposure resolved the large 120 kDa band in the AT-FL-65Q sample lane into two distinct bands. High-molecular weight (>200 kDa) bands and high-molecular weight smearing were seen in both DRPLA patients and AT-FL-65Q mice. A single band at  $\sim$ 200 kDa was seen in the control nuclear extracts. Labeling of the blots with antibodies to poly-ADP-ribose polymerase (a mostly nuclear protein) and glyceraldehyde 3-phosphate dehydrogenase (a mostly cytoplasmic protein) confirmed the efficiency of separation into nuclear and cytoplasmic fractions (data not shown). Details regarding the patient and control tissues are provided in the Experimental Procedures.

the symptoms of which include tremors and other abnormal movements, ataxia, incoordination, seizures, and premature death. The brains of these animals appear grossly normal, but nuclei of multiple neuronal populations accumulate aberrant atrophin-1 immunoreactivity and atrophin-1-immunoreactive inclusions. The temporal and spatial distribution of nuclear atrophin-1 immunoreactivity correlated with the appearance and accumulation of 120 kDa fragments of mutant protein. The appearance of the 120 kDa fragments precedes the appearance of overt behavioral symptoms, and the levels of the fragments increase as the course of the disease progresses. Apparently identical fragments of mutant atrophin-1 were detected, albeit at lower levels, in nuclear extracts from cerebella of DRPLA patients. In addition to the 120 kDa fragments, higher-molecular weight bands (>200 kDa) and smearing of immunoreactivity were observed in all AT-FL-65Q brain nuclear preparations. The higher bands could result from the action of transglutaminases or from covalent modification with ubiquitin-like molecules, while the smearing probably results from polyglutamine-mediated aggregation. Collectively, these data suggest that nuclear accumulation of truncated mutant atrophin-1 protein plays a role in the evolution of neuropathology in DRPLA.

DRPLA patients have neuronal degeneration in a number of brain areas and widespread distribution of ubiquitinated neuronal and glial intranuclear inclusions in the brain (Hayashi et al., 1998). Our mutant atrophin-1 transgenic mice show a similar widespread distribution of nuclear pathology. Although we do not observe severe degeneration of the dentate of the cerebellum or globus pallidus, two regions heavily affected in DRPLA, it is possible that more subtle losses have occurred.

Studies are underway using stereologic counting procedures to assess the numbers of neurons in mice at various ages in relevant neuronal populations. We anticipate that these investigations will determine the extent of neuronal loss.

As has been described in HD and DRPLA patients and transgenic models of HD (Mangiarini et al., 1996; Davies et al., 1997; DiFiglia et al., 1997; Becher et al., 1998; Hayashi et al., 1998; Igarashi et al., 1998; Reddy et al., 1998; Schilling et al., 1999), we demonstrate neuronal intranuclear inclusions in multiple populations of neurons in our mutant atrophin-1 mice. These inclusions are thought to consist of aggregates of the expanded polyglutamine protein; aggregation may be driven through polar zippers (Perutz, 1995; Scherzinger et al., 1997) and stabilized by the action of transglutaminases (Igarashi et al., 1998; Kahlem et al., 1998). Other proteins such as caspases, chaperones, proteasomes, and proteins containing long stretches of glutamines (tata-binding protein [TBP], for example) can be recruited into inclusions (Cummings et al., 1998; Perez et al., 1998; Chai et al., 1999; Sanchez et al., 1999; Stenoien et al., 1999). However, the inclusions per se may not be toxic, and other forms of mutant protein may represent the toxic entity (Klement et al., 1998; Saudou et al., 1998; Gutekunst et al., 1999).

#### A Possible Role for Proteolytic Processing in the Pathogenesis of Polyglutamine Diseases

Proteolytic processing of polyglutamine proteins has been hypothesized to play a role in the pathogenesis of disorders caused by expansions of glutamine repeats (Goldberg et al., 1996; Ikeda et al., 1996; Miyashita et al., 1997; Ross, 1997; Wellington et al., 1998; Ellerby et al., 1999a, 1999b). HD postmortem brain appears to contain truncated fragments of huntingtin (DiFiglia et al., 1997; Becher et al., 1998), which may result from the action of caspases (Goldberg et al., 1996; Wellington et al., 1998) or other proteases. In cultured cells, truncated fragments of huntingtin and other polyglutamine-containing proteins are often more toxic and more likely to aggregate into polymeric structures (Cooper et al., 1998; Martindale et al., 1998; Moulder et al., 1999). Transgenic mice expressing N-terminal fragments of huntingtin develop behavioral and neuropathological features that resemble aspects of HD (Mangiarini et al., 1996; Davies et al., 1997; Schilling et al., 1999). A yeast artificial chromosome transgenic model of HD has intranuclear huntingtin immunoreactivity using antibodies to the N terminus but not to an internal epitope (Hodgson et al., 1999). Collectively, these observations have given rise to the toxic fragment hypothesis, whereby smaller proteolytic fragments of expanded polyglutamine proteins containing the glutamine repeat show a greater propensity for aggregation and may underlie neuronal dysfunction and the neurological phenotype (Ikeda et al., 1996; DiFiglia et al., 1997; Ross, 1997; Davies et al., 1998).

However, previous studies have seen fragments on Western blots only inconsistently (DiFiglia et al., 1997) or have relied on differential antibody reactivity to different epitopes by immunohistochemistry (DiFiglia et al., 1997; Becher et al., 1998; Hodgson et al., 1999), which can be difficult to interpret due to the possibility of antigen

masking in aggregates. The present report provides evidence of aberrant accumulation and aggregation of truncated fragments of mutant atrophin-1 in a transgenic mouse model of DRPLA. Seemingly identical fragments were observed in DRPLA patients. An alternative possibility is that the 120 kDa bands represent full-length atrophin-1 that is not modified in the same way that atrophin-1 normally is, perhaps because there is less of the modifying protein(s) in the nucleus. However, previous studies of atrophin-1, using different antibodies, have also described it as running at 150–180 kDa (Knight et al., 1997; Yazawa et al., 1995; Miyashita et al., 1998). In addition, *in vitro* transcription and translation also yield a single band at 150–180 kDa (Miyashita et al., 1997; Wellington et al., 1998).

Because of the strong correlation between the levels of the fragments and the levels of pathologic nuclear immunoreactivity, we believe that the generation of the fragments contributes to the evolution of pathology. Preliminary studies in transfected N2a cells suggest that C-terminally truncated atrophin-1 fragments, including 65Q, are more toxic to cells than the full-length atrophin-1 with 65Q (F. Nucifora et al., personal communication). Thus, there is reason to believe that the 120 kDa fragments may be more toxic than the full-length protein.

The nature of the proteolytic event that gives rise to the 120 kDa mutant fragments has yet to be defined. A number of polyglutamine proteins, including atrophin-1 and huntingtin, are subject to cleavage *in vitro* by members of the caspase family of endoproteases (Goldberg et al., 1996; Wellington et al., 1998; Ellerby et al., 1999a, 1999b), and thus the appearance of the fragments and their increase in abundance as the mutant mice age may be a consequence of cellular dysfunction and caspase activation. However, our analysis of the 26Q mice indicates that atrophin-1 may normally be subject to proteolytic processing, generating fragments of 120 kDa and larger (see Figure 2B). Thus, the production of the 120 kDa fragments may be a normal event in the processing or degradation of atrophin-1 and not a nonspecific consequence of the activation of proteases associated with cell death.

An analysis of amino acid sequence motifs in atrophin-1 identified a motif in the N terminus (residues 16–32) with homology to nuclear localization signals (NLS) and a motif near the C terminus (residues 1033–1041) with homology to nuclear export signals (NES). Immunoblotting with an N-terminal peptide antibody indicated that the 120 kDa fragments contain the N terminus (J. W., unpublished data). Thus, on the basis of the relative molecular mass of the 120 kDa fragments, we believe that the putative NES would be removed and that the truncation could alter the normal location of the protein to favor a nuclear localization. Preliminary studies suggest that both the NLS and NES are functional (F. Nucifora, personal communication).

One important aspect of our analysis of the 120 kDa fragments was the notable increase in their abundance in the mutant mice as a function of age. Without knowledge of the relative half-lives of the full-length mutant protein and the 120 kDa fragments, it is difficult to know whether the increased abundance of the fragments as the animals age is a consequence of an accumulation of the fragments over time or increased generation of

the fragments. We favor a scenario in which truncation of mutant atrophin-1 creates a molecule that is much longer lived than full-length protein because it is (1) preferentially mislocalized to the nucleus and (2) more prone to aggregate into nondegradable structures. In this setting, the increase in the abundance of the mutant 120 kDa fragments as the 65Q mice age would be the consequence of its accumulation over time.

Our immunocytochemical and biochemical analyses of the mutant mice clearly demonstrate that the 120 kDa fragments are localized to the nucleus. Other studies have recently identified the nucleus as a critical site for toxicity of polyglutamine proteins (Klement et al., 1998; Saudou et al., 1998; Peters et al., 1999). Ataxin-1 and ataxin-3 associate with proteins present in the nuclear matrix (Matilla et al., 1997; Skinner et al., 1997; Tait et al., 1998). The question arises as to what processes are affected by the nuclear accumulation of truncated atrophin-1 fragments. We have recently found that the N terminus of atrophin-1 interacts with ETO, a component of nuclear corepressor complexes localized to the nuclear matrix (J. W., unpublished data). This raises the possibility that the regulation of transcription is altered.

### Conclusions

In summary, our study demonstrates that truncated products of mutant atrophin-1 are found in mutant transgenic mice and in the cerebella of DRPLA cases. The temporal and spatial distribution of these fragments correlates well with the appearance of aberrant nuclear atrophin-1 immunoreactivity and atrophin-1 immunoreactive inclusions in the nucleus of multiple neuronal populations. Our mutant atrophin-1 transgenic mice represent a polyglutamine disease animal model that clearly demonstrates proteolytic fragments of the mutant polyglutamine protein. We propose that this is an important event in the evolution of pathological changes. Although the levels of these fragments in human tissues seemed to be lower than the levels in mice, the extent of cell loss in the human cases may be much greater than in the mice, and the expression profiles of the atrophin-1 and prion protein promoters may differ. Furthermore, nuclear fractionation of postmortem tissues is significantly more difficult than fractionating fresh tissues from the mice. Thus, we believe that the accumulation of the truncated atrophin-1 molecules found in the mutant mice is an authentic recapitulation of events occurring in the human disease. These mice will prove a source of tissue that will help characterize the nature of the proteolytic processing that generates the 120 kDa mutant fragments and for defining the role of these molecules in the pathogenesis of disease.

### Experimental Procedures

#### Transgene Construction

Full-length cDNAs of *atrophin-1* encoding 26 and 65 consecutive glutamines were constructed as described elsewhere (Margolis et al., 1996). These constructs contain ~70 nucleotides of *atrophin-1* 5'-UTR and ~600 nucleotides of 3'-UTR. The *atrophin-1* cDNAs were excised with KpnI and XbaI, blunt ended, and flanked with phosphorylated XhoI linkers (Stratagene; 5'-CCGCTCGAGCGG-3'). They were then digested with XhoI and ligated into the mouse prion

protein promoter vector (Borchelt et al., 1996). The transgene constructs were transfected into HEK293 cells, and protein expression was confirmed by Western blot analysis. The constructs were linearized with NotI and resolved on a 0.6% low-melting point agarose gel (FMC Bioproducts). The agarose was digested with  $\beta$ -agarase (Epicentre Technologies), and after further purification, DNA was injected into the male pronucleus of fertilized oocytes. Founders were analyzed for insertion of the transgene with a three-way PCR reaction with the following primers: PrP-sense (5'-CCTCTTTGTGAC TATGTGGACTGATGTCGG5-3') and PrP-antisense (5'-GTGGATAC CCCCTCCCCAGCCTAGACC-3'), which together give a product of 700 bp, and At-3818-5' (5'-AGGTGGGAGGTGGCGAGGAT-3'), which gives a transgene-specific product of 400 bp with PrP-antisense in transgenic animals. The copy number was established by probing of a Southern blot of genomic mouse tail DNA with random prime-labeled BamHI fragments of atrophin-1 (bp 2980-3348). Animals with more than ten copies were bred into stable transgenic lines. The lines were maintained on a hybrid C3H/B6 background (Jackson Laboratories).

#### Northern Blot Analysis

Transgene expression in the breeding lines was analyzed by Northern blot. Total RNA was prepared from mouse brains with TRIZOL (BRL), and 5  $\mu$ g of total RNA was fractionated on a formaldehyde agarose gel. RNA was transferred to a nylon membrane (GeneScreen; NEN) and probed with a random prime-labeled BamHI fragment of human atrophin-1 (bp 2980-3348). The Northern blot was re-probed with a <sup>32</sup>P-labeled fragment of PrP to verify equal loading of RNA in each lane.

#### Human Tissue Samples

Frozen pieces of cerebella from the following cases were used. DRPLA cases: N17(81) (female; 66Q; onset, 8 years; duration, 9 years), N11(96) (female; 65Q; onset, 14 years; duration, 18 years), and N8(98) (male; 67Q; onset, 16 years; duration, 13 years); control cases: N2(98) (male; death, 56 years) and N28(98) (female; death, 74 years).

#### Preparation of Nuclei and Cytosol

Brain tissue was homogenized in 15 volumes (w/v) of 0.25 M sucrose/buffer A (50 mM triethanolamine [pH 7.5], 25 mM KCl, 5 mM MgCl<sub>2</sub>, 0.5 mM dithiothreitol, and 0.5 mM phenylmethylsulfonyl [PMSF], supplemented with Complete protease inhibitor cocktail tablets [Boehringer Mannheim]) and centrifuged at 800  $\times$  g for 15 min at 4°C. The supernatants were centrifuged at 100,000  $\times$  g for 1 hr at 4°C, and the resulting supernatants were taken as the cytosolic fractions (C). The pellets from the initial centrifugation step were resuspended in 10 ml each of 0.25 M sucrose/buffer A and then mixed with 20 ml each of 2.3 M sucrose/buffer A. The resulting mixtures were layered on top of 10 ml each of 2.3 M sucrose/buffer A, and then nuclei were pelleted by centrifugation at 12,400  $\times$  g for 1 hr at 4°C. The pellet was resuspended in 0.25 M sucrose/buffer A and washed by low-speed centrifugation. The final pellet was designated as the nuclear fraction (N).

#### Immunoblot Analysis

Protein concentrations were assayed by the dye-binding method (Pierce) with bovine serum albumin as standard. Cytosol samples were concentrated by trichloroacetic acid precipitation when necessary, and proteins were solubilized in SDS-PAGE loading buffer at 0.5  $\mu$ g.ml<sup>-1</sup>. They were then sonicated for 20 s, heated at 70°C for 5 min, and microfuged for 1 min prior to loading. Proteins were resolved by SDS-PAGE in a 6% polyacrylamide-SDS gel at 10 mA per gel and then transferred to a polyvinylidene difluoride membrane (Schleicher and Schuell). Transfer buffer was 25 mM Tris, 192 mM glycine, 0.1% SDS, and 10% methanol; the inclusion of SDS in the transfer buffer was found to greatly enhance atrophin-1 signal strength. Immunoblots were probed with anti-atrophin-1 antibody AP142 (Wood et al., 1998). Bound antibodies were visualized with horseradish peroxidase-conjugated secondary antibodies and enhanced chemiluminescence (Renaissance; NEN). Identically loaded gels were stained with Coomassie blue to confirm equivalent protein loadings.

To analyze the distribution of mutant atrophin-1 expression, mouse brains were dissected on an ice-cold glass plate, and specific regions from different mice were pooled. The regions were homogenized in 15 volumes (w/v) of 5 mM HEPES (pH 7.4), 0.32 M sucrose, and 0.1 mM PMSF, supplemented with Complete protease inhibitor cocktail (Boehringer Mannheim). Crude postnuclear (P1) pellets were prepared by centrifugation at  $500 \times g$  for 5 min at 4°C. These were resuspended in one third of the volume of buffer used for homogenization, assayed for protein concentration, and subjected to immunoblot analysis as above. Identically loaded gels were stained with Coomassie blue to confirm equivalent protein loadings. Although the mouse prion promoter has been shown to express in heart (Borchelt et al., 1996), atrophin-1 transgene products were not detected in this tissue by immunoblotting (data not shown).

#### Immunocytochemistry

Animals were anesthetized in methoxyflurane (Metofane; Mallinckrodt Veterinary) and perfused with periodate lysine paraformaldehyde (PLP) (2% paraformaldehyde, 75 mM lysine, and 10 mM sodium periodate in phosphate-buffered saline [PBS]) through the left cardiac ventricle. The brains were removed, postfixed in PLP overnight, and then transferred to PBS. The brains were cut sagittally and processed for paraffin embedding. Immunostaining of sections (8  $\mu$ m) was done with AP142 (Wood et al., 1998) at a dilution of 1:10,000 or 1:25,000 following standard protocols.

#### Rotating Rod Analysis

Six naive animals of lines AT-FL-65Q-150 and AT-FL-26Q-79 and six nontransgenic mice were tested on an accelerating rotating rod (Rotamex 4/8; Columbus Instruments International). The speed of the rod was set to increase from 4 revolutions per min to 40 revolutions per min over a 10 min period. The amount of time it took for the mice to fall from the rod was measured in four trials per day over a 4 day period. At least 10 min of recovery time was allowed between trials. The data for each group of animals were averaged.

#### Acknowledgments

This work was supported by the Hereditary Disease Foundation, the Huntington's Disease Society of America Coalition for the Cure, and by the National Institutes of Health (grants NS34172 and NS16375), the DeVelbiss Fund, and a bequest from the estate of Sar and Brita Levitan.

Received May 18, 1999; revised July 7, 1999.

#### References

Banfi, S., Servadio, A., Chung, M.Y., Kwiatkowski, T.J., Jr., McCall, A.E., Duvick, L.A., Shen, Y., Roth, E.J., Orr, H.T., and Zoghbi, H.Y. (1994). Identification and characterization of the gene causing type 1 spinocerebellar ataxia. *Nat. Genet.* **7**, 513–520.

Becher, M.W., Rubinsztein, D.C., Leggo, J., Wagster, M.V., Stine, O.C., Ranen, N.G., Franz, M.L., Abbott, M.H., Sherr, M., MacMillan, J.C. et al. (1997). Dentatorubral and pallidolusian atrophy (DRPLA). Clinical and neuropathological findings in genetically confirmed North American and European pedigrees. *Mov. Disord.* **12**, 519–530.

Becher, M.W., Kotzok, J.A., Sharp, A.H., Davies, S.W., Bates, G.P., Price, D.L., and Ross, C.A. (1998). Intranuclear neuronal inclusions in Huntington's disease and dentatorubral and pallidolusian atrophy: correlation between the density of inclusions and IT15 CAG triplet repeat length. *Neurobiol. Dis.* **4**, 387–397.

Borchelt, D.R., Davis, J., Fischer, M., Lee, M.K., Slunt, H.H., Ratovitsky, T., Regard, J., Copeland, N.G., Jenkins, N.A., Sisodia, S.S., and Price, D.L. (1996). A vector for expressing foreign genes in the brains and hearts of transgenic mice. *Genet. Anal.* **13**, 159–163.

Chai, Y., Koppenhafer, S.L., Shoesmith, S.J., Perez, M.K., and Paulson, H.L. (1999). Evidence for proteasome involvement in polyglutamine disease: localization to nuclear inclusions in SCA3/MJD and

suppression of polyglutamine aggregation in vitro. *Hum. Mol. Genet.* **8**, 673–682.

Cooper, J.K., Schilling, G., Peters, M.F., Herring, W.J., Sharp, A.H., Kaminski, Z., Masone, J., Khan, F.A., Delaney, M., Borchelt, D.R., Dawson, V.L., Dawson, T.M., and Ross, C.A. (1998). Truncated N-terminal fragments of huntingtin with expanded glutamine repeats form nuclear and cytoplasmic aggregates in cell culture. *Hum. Mol. Genet.* **7**, 793–790.

Cummings, C.J., Mancini, M.A., Antalffy, B., DeFranco, D.B., Orr, H.T., and Zoghbi, H.Y. (1998). Chaperone suppression of aggregation and altered subcellular proteasome localization imply protein misfolding in SCA1. *Nat. Genet.* **19**, 148–154.

Davies, S.W., Turmaine, M., Cozens, B.A., DiFiglia, M., Sharp, A.H., Ross, C.A., Scherzinger, E., Wanker, E.E., Mangiarini, L., and Bates, G.P. (1997). Formation of neuronal intranuclear inclusions underlies the neurological dysfunction in mice transgenic for the HD mutation. *Cell* **90**, 537–548.

Davies, S.W., Beardsall, K., Turmaine, M., DiFiglia, M., Aronin, N., and Bates, G.P. (1998). Are neuronal intranuclear inclusions the common neuropathology of triplet-repeat disorders with polyglutamine-repeat expansions? *Lancet* **351**, 131–133.

DiFiglia, M., Sapp, E., Chase, K.O., Davies, S.W., Bates, G.P., Vonsattel, J.P., and Aronin, N. (1997). Aggregation of huntingtin in neuronal intranuclear inclusions and dystrophic neurites in brain. *Science* **277**, 1990–1993.

Ellerby, L.M., Hackam, A.S., Propp, S.S., Ellerby, H.M., Rabizadeh, S., Cashman, N.R., Trifiro, M.A., Pinsky, L., Wellington, C.L., Salvesen, G.S. et al. (1999a). Kennedy's disease: caspase cleavage of the androgen receptor is a crucial event in cytotoxicity. *J. Neurochem.* **72**, 185–195.

Ellerby, L.M., Andrusiak, R.L., Wellington, C.L., Hackam, A.S., Propp, S.S., Wood, J.D., Sharp, A.H., Margolis, R.L., Ross, C.A., Salvesen, G.S. et al. (1999b). Cleavage of atrophin-1 at caspase site aspartic acid 109 modulates cytotoxicity. *J. Biol. Chem.* **274**, 8730–8736.

Goldberg, Y.P., Nicholson, D.W., Rasper, D.M., Kalchman, M.A., Koide, H.B., Graham, R.K., Bromm, M., Kazemi-Esfarjani, P., Thornberry, N.A., Vaillancourt, J.P., and Hayden, M.R. (1996). Cleavage of huntingtin by apopain, a proapoptotic cysteine protease, is modulated by the polyglutamine tract. *Nat. Genet.* **13**, 442–449.

Gusella, J.F., and MacDonald, M.E. (1996). Trinucleotide instability: a repeating theme in human inherited disorders. *Annu. Rev. Med.* **47**, 201–209.

Gutkunst, C.A., Li, S.H., Yi, H., Mulroy, J.S., Kuemmerle, S., Jones, R., Rye, D., Ferrante, R.J., Hersch, S.M., and Li, X.J. (1999). Nuclear and neuropil aggregates in Huntington's disease: relationship to neuropathology. *J. Neurosci.* **19**, 2522–2534.

Hayashi, Y., Kakita, A., Yamada, M., Koide, R., Igarashi, S., Takano, H., Ikeuchi, T., Wakabayashi, K., Egawa, S., Tsuji, S., and Takahashi, H. (1998). Hereditary dentatorubral-pallidolusian atrophy: detection of widespread ubiquitinated neuronal and glial intranuclear inclusions in the brain. *Acta Neuropathol. (Berl)* **96**, 547–552.

Hodgson, G.J., Agopyan, N., Gutkunst, C.A., Leavitt, B.R., LePiane, F., Singaraja, R., Smith, D.J., Bissada, N., McCutcheon, K., Nassir et al. (1999). A YAC mouse model for Huntington's disease with full-length mutant huntingtin, cytoplasmic toxicity, and selective striatal neurodegeneration. *Neuron* **23**, 1–12.

The Huntington's Disease Collaborative Research Group (1993). A novel gene containing a trinucleotide repeat that is expanded and unstable on Huntington's disease chromosomes. *Cell* **72**, 971–983.

Igarashi, S., Koide, R., Shimohata, T., Yamada, M., Hayashi, Y., Takano, H., Date, H., Oyake, M., Sato, T., Sato, A. et al. (1998). Suppression of aggregate formation and apoptosis by transglutaminase inhibitors in cells expressing truncated DRPLA protein with an expanded polyglutamine stretch. *Nat. Genet.* **18**, 111–117.

Izuka, R., Hirayama, K., and Maehara, K. (1984). Dentato-rubro-pallido-lusian atrophy: a clinico-pathological study. *J. Neurol. Neurosurg. Psychiatry* **47**, 1288–1298.

Ikedo, H., Yamaguchi, M., Sugai, S., Aze, Y., Narumiya, S., and Kakizuka, A. (1996). Expanded polyglutamine in the Machado-Joseph disease protein induces cell death in vitro and in vivo. *Nat. Genet.* **13**, 196–202.

- Ikeuchi, T., Koide, R., Tanaka, H., Onodera, O., Igarashi, S., Takahashi, H., Kondo, R., Ishikawa, A., Tomoda, A., Miike, T. et al. (1995). Dentatorubral-pallidolusian atrophy: clinical features are closely related to unstable expansions of trinucleotide (CAG) repeat. *Ann. Neurol.* *37*, 769–775.
- Kahlem, P., Green, H., and Djian, P. (1998). Transglutaminase action imitates Huntington's disease: selective polymerization of Huntingtin containing expanded polyglutamine. *Mol. Cell.* *1*, 595–601.
- Klement, I.A., Skinner, P.J., Kaytor, M.D., Yi, H., Hersch, S.M., Clark, H.B., Zoghbi, H.Y., and Orr, H.T. (1998). Ataxin-1 nuclear localization and aggregation: role in polyglutamine-induced disease in SCA1 transgenic mice. *Cell* *95*, 41–53.
- Knight, S.P., Richardson, M.M., Osmand, A.P., Stakkestad, A., and Potter, N.T. (1997). Expression and distribution of the dentatorubral-pallidolusian atrophy gene product (atrophin-1/drplap) in neuronal and non-neuronal tissues. *J. Neurol. Sci.* *146*, 19–26.
- Koide, R., Ikeuchi, T., Onodera, O., Tanaka, H., Igarashi, S., Endo, K., Takahashi, H., Kondo, R., Ishikawa, A., Hayashi, T. et al. (1994). Unstable expansion of CAG repeat in hereditary dentatorubral-pallidolusian atrophy (DRPLA). *Nat. Genet.* *6*, 9–13.
- Komure, O., Sano, A., Nishino, N., Yamauchi, N., Ueno, S., Kondoh, K., Sano, N., Takahashi, M., Murayama, N., Kondo, I. et al. (1995). DNA analysis in hereditary dentatorubral-pallidolusian atrophy: correlation between CAG repeat length and phenotypic variation and the molecular basis of anticipation. *Neurology* *45*, 143–149.
- Li, S.H., McInnis, M.G., Margolis, R.L., Antonarakis, S.E., and Ross, C.A. (1993). Novel triplet repeat containing genes in human brain: cloning, expression, and length polymorphisms. *Genomics* *16*, 572–579.
- Mangiarini, L., Sathasivam, K., Seller, M., Cozens, B., Harper, A., Hetherington, C., Lawton, M., Trotter, Y., Lehrach, H., Davies, S.W., and Bates, G.P. (1996). Exon 1 of the *HD* gene with an expanded CAG repeat is sufficient to cause a progressive neurological phenotype in transgenic mice. *Cell* *87*, 493–506.
- Margolis, R.L., Li, S.H., Young, W.S., Wagster, M.V., Stine, O.C., Kidwai, A.S., Ashworth, R.G., and Ross, C.A. (1996). DRPLA gene (atrophin-1) sequence and mRNA expression in human brain. *Brain Res. Mol. Brain Res.* *36*, 219–226.
- Martindale, D., Hackam, A., Wiczorek, A., Ellerby, L., Wellington, C., McCutcheon, K., Singaraja, R., Kazemi-Esfarjani, P., Devon, R., Kim, S.U., et al. (1998). Length of huntingtin and its polyglutamine tract influences localization and frequency of intracellular aggregates. *Nat. Genet.* *18*, 150–154.
- Matilla, A., Koshy, B.T., Cummings, C.J., Isobe, T., Orr, H.T., and Zoghbi, H.Y. (1997). The cerebellar leucine-rich acidic nuclear protein interacts with ataxin-1. *Nature* *389*, 974–978.
- Miyashita, T., Okamura-Oho, Y., Mito, Y., Nagafuchi, S., and Yamada, M. (1997). Dentatorubral pallidolusian atrophy (DRPLA) protein is cleaved by caspase-3 during apoptosis. *J. Biol. Chem.* *272*, 29238–29242.
- Miyashita, T., Nagao, K., Ohmi, K., Yanagisawa, H., Okamura-Oho, Y., and Yamada, M. (1998). Intracellular aggregate formation of dentatorubral-pallidolusian atrophy (DRPLA) protein with the extended polyglutamine. *Biochem. Biophys. Res. Commun.* *249*, 96–102.
- Moulder, K.L., Onodera, O., Burke, J.R., Strittmatter, W.J., and Johnson, E.M., Jr. (1999). Generation of neuronal intranuclear inclusions by polyglutamine-GFP: analysis of inclusion clearance and toxicity as a function of polyglutamine length. *J. Neurosci.* *19*, 705–715.
- Nagafuchi, S., Yanagisawa, H., Ohsaki, E., Shirayama, T., Tadokoro, K., Inoue, T., and Yamada, M. (1994a). Structure and expression of the gene responsible for the triplet repeat disorder, dentatorubral and pallidolusian atrophy (DRPLA). *Nat. Genet.* *8*, 177–182.
- Nagafuchi, S., Yanagisawa, H., Sato, K., Shirayama, T., Ohsaki, E., Bundo, M., Takeda, T., Tadokoro, K., Kondo, I., Murayama, N. et al. (1994b). Dentatorubral and pallidolusian atrophy expansion of an unstable CAG trinucleotide on chromosome 12p. *Nat. Genet.* *6*, 14–18.
- Naito, H., and Oyanagi, S. (1982). Familial myoclonus epilepsy and choreoathetosis: hereditary dentatorubral-pallidolusian atrophy. *Neurology* *32*, 798–807.
- Orr, H.T., Chung, M.Y., Banfi, S., Kwiatkowski, T.J., Jr., Servadio, A., Beaudet, A.L., McCall, A.E., Duvick, L.A., Ranum, L.P., and Zoghbi, H.Y. (1993). Expansion of an unstable trinucleotide CAG repeat in spinocerebellar ataxia type 1. *Nat. Genet.* *4*, 221–226.
- Paulson, H.L., and Fischbeck, K.H. (1996). Trinucleotide repeats in neurogenetic disorders. *Annu. Rev. Neurosci.* *19*, 79–107.
- Perez, M.K., Paulson, H.L., Pendse, S.J., Saionz, S.J., Bonini, N.M., and Pittman, R.N. (1998). Recruitment and the role of nuclear localization in polyglutamine-mediated aggregation. *J. Cell. Biol.* *143*, 1457–1470.
- Perutz, M.F. (1995). Glutamine repeats as polar zippers: their role in inherited neurodegenerative disease. *Mol. Med.* *1*, 718–721.
- Peters, M.F., Nucifora, F.C., Kushi, J., Seaman, H., Cooper, J.K., Herring, W.J., Dawson, V.L., Dawson, T.M., and Ross, C.A. (1999). Nuclear targeting of mutant Huntingtin increases toxicity. *Mol. Cell. Neurosci.*, in press.
- Reddy, P.H., Williams, M., Charles, V., Garrett, L., Pike-Buchanan, L., Whetsell, W.O., Jr., Miller, G., and Tagle, D.A. (1998). Behavioural abnormalities and selective neuronal loss in HD transgenic mice expressing mutated full-length HD cDNA. *Nat. Genet.* *20*, 198–202.
- Ross, C.A. (1997). Intranuclear neuronal inclusions: a common pathogenic mechanism for glutamine-repeat neurodegenerative diseases? *Neuron* *19*, 1147–1150.
- Ross, C.A., Becher, M.W., Colomer, V., Engelender, S., Wood, J.D., and Sharp, A.H. (1997a). Huntington's disease and dentatorubral-pallidolusian atrophy: proteins, pathogenesis and pathology. *Brain Pathol.* *7*, 1003–1016.
- Ross, C.A., Margolis, R.L., Rosenblatt, A., Ranen, N.G., Becher, M.W., and Aylward, E. (1997b). Huntington disease and the related disorder, dentatorubral-pallidolusian atrophy (DRPLA). *Medicine (Baltimore)* *76*, 305–338.
- Sanchez, I., Xu, C.J., Juo, P., Kakizaka, A., Blenis, J., and Yuan, J. (1999). Caspase-8 is required for cell death induced by expanded polyglutamine repeats. *Neuron* *22*, 623–633.
- Saudou, F., Finkbeiner, S., Devys, D., and Greenberg, M.E. (1998). Huntingtin acts in the nucleus to induce apoptosis but death does not correlate with the formation of intranuclear inclusions. *Cell* *95*, 55–66.
- Scherzinger, E., Lurz, R., Turmaine, M., Mangiarini, L., Hollenbach, B., Hasenbank, R., Bates, G.P., Davies, S.W., Lehrach, H., and Wanker, E.E. (1997). Huntingtin-encoded polyglutamine expansions form amyloid-like protein aggregates in vitro and in vivo. *Cell* *90*, 549–558.
- Schilling, G., Becher, M.W., Sharp, A.H., Jinnah, H.A., Duan, K., Kotzok, J.A., Slunt, H.H., Ratovitski, T., Cooper, J.K., Jenkins, N.A. et al. (1999). Intranuclear inclusions and neuritic pathology in transgenic mice expressing a mutant N-terminal fragment of huntingtin. *Hum. Mol. Genet.* *8*, 397–407.
- Skinner, P.J., Koshy, B.T., Cummings, C.J., Klement, I.A., Helin, K., Servadio, A., Zoghbi, H.Y., and Orr, H.T. (1997). Ataxin-1 with an expanded glutamine tract alters nuclear matrix-associated structures. *Nature* *389*, 971–974.
- Smith, J.K., Gonda, V.E., and Malamud, N. (1958). Unusual form of cerebellar ataxia: combined dentato-rubral and pallido-lusian degeneration. *Neurology* *8*, 205–209.
- Stenoien, D.L., Cummings, C.J., Adams, H.P., Mancini, M.G., Patel, K., DeMartino, G.N., Marcelli, M., Weigel, N.L., and Mancini, M.A. (1999). Polyglutamine-expanded androgen receptors form aggregates that sequester heat shock proteins, proteasome components and SRC-1, and are suppressed by the HDJ-2 chaperone. *Hum. Mol. Genet.* *8*, 731–741.
- Tait, D., Riccio, M., Sittler, A., Scherzinger, E., Santi, S., Ognibene, A., Maraldi, N.M., Lehrach, H., and Wanker, E.E. (1998). Ataxin-3 is transported into the nucleus and associates with the nuclear matrix. *Hum. Mol. Genet.* *7*, 991–997.
- Takahashi, H., Ohama, E., Naito, H., Takeda, S., Nakashima, S., Makifuchi, T., and Ikuta, F. (1988). Hereditary dentatorubral-pallidolusian atrophy: clinical and pathologic variants in a family. *Neurology* *38*, 1065–1070.
- Trotter, Y., Devys, D., Imbert, G., Saudou, F., An, I., Lutz, Y., Weber,

C., Agid, Y., Hirsch, E.C., and Mandel, J.L. (1995). Cellular localization of the Huntington's disease protein and discrimination of the normal and mutated form. *Nat. Genet.* *10*, 104–110.

Wellington, C.L., Ellerby, L.M., Hackam, A.S., Margolis, R.L., Trifiro, M.A., Singaraja, R., McCutcheon, K., Salvesen, G.S., Propp, S.S., Bromm, M. et al. (1998). Caspase cleavage of gene products associated with triplet expansion disorders generates truncated fragments containing the polyglutamine tract. *J. Biol. Chem.* *273*, 9158–9167.

Wood, J.D., Yuan, J., Margolis, R.L., Colomer, V., Duan, K., Kushi, J., Kaminsky, Z., Kleiderlein, J.J., Sharp, A.H., and Ross, C.A. (1998). Atrophin-1, the DRPLA gene product, interacts with two families of WW domain-containing proteins. *Mol. Cell. Neurosci.* *11*, 149–160.

Yazawa, I., Nukina, N., Hashida, H., Goto, J., Yamada, M., and Kanazawa, I. (1995). Abnormal gene product identified in hereditary dentatorubral-pallidolusian atrophy (DRPLA) brain. *Nat. Genet.* *10*, 99–103.